American Journal of Engineering Research (AJER) **2017**
American Journal of Engineering Research (AJER)
e-ISSN: 2320-0847 p-ISSN : 2320-0936
Volume-6, Issue-7, pp-347-363
www.ajer.org
Research Paper Open Access

Performane Assessment of Unreinforced Masonry Low-Rise Building Composed of Limestone Bricks Under Seismic Loading

[*]Mohamed Gamaleldeen Elsayem[1], Abdelsalam Ahmed Mokhtar[2], Gamal Hussein[2] ,Mahmoud Elghorab[3], Mohamed Kohail [3]
[1,2,3] *Assistant lecturer, Professor and Assistant Professor,*
*Corresponding Author: *Mohamed Gamaleldeen Elsayem*
Structural Engineering Department, Faculty of Engineering, Ain Shams University, Cairo, Egypt

ABSTRACT: This paper demonstrates the analytical investigations of the nonlinear behavior of entirely limestone unreinforced masonry structure (URM) composed of barrel vaults rested on wall bearing under seismic loading where the nonlinearity mean the ultimate capacity. Usually, linear analysis is conducted for simplifying analysis and design of masonry structures by using load and strength factors. However, such simplification might underestimate the structural capacity of these constructions in many cases, and thus the nonlinear analysis gives better description for the actual behavior and capacity of the structure. The finite Element Program (Abaqus) was used to analysis the proposed limestone URM building.

Keywords: Limestone, Barrel Vaults, Unreinforced Masonry, URM, Seismic Behavior, In-plane Seismic Record, Economic Housing, Value Engineering.

Date of Submission: 17 -05-2017 Date of acceptance: 20-07-2017

I. INTRODUCTION

Masonry structures are widespread in the world, build with different materials and different masonry techniques. Some of them are old: masonry construction initiated in the ancient times, as early as 4.000 BC with stonemasonry in Ancient Egypt, and culminated in the Roman era with the development of the Roman Arch. Masonry buildings are affected by the materials used, the quality of the mortar and workmanship, the assembly, and their age. Although superseded by concrete construction in the 20th century, there are numerous masonry residential buildings still used for housing. Many historic masonry building are still existing and resisting all types of the seismic, temperature and wind load. Many researchers were monitoring and evaluating the state of these historic buildings [1, 2]. In Egypt, tens of millions of people can't afford a new RC building. The unreinforced masonry system URM is considered a promising economic alternative [3, 4]

for the low-rise building instead of traditional RC skeleton systems due to many factors. First, no need for pouring concrete for columns or beams or slabs in-situ. Second, no need for plastering or paintings. Third, the durability of natural materials like stone bricks is higher than reinforced concrete or steel structures. Forth, the capability of increasing the rate of construction is by increasing the labors in-situ. Fifth, these masonry units can resist high temperature due to its large thermal resistance which is less consumption of electric energy power. Sixth, it helps achieving the sustainability concept by using an widespread environmental material in Egypt like Limestone without an expensive industry costs or consuming large energy in its manufacturing process.

A lot of research experimentally tested full-scale URM building subjected to lateral dynamic loads to simulate the earthquake hazards [5, 6, 7, 8]. In our case study, the proposed limestone URM building was expected to be a better alternative rather than either RC or Steel structures for constructing many low-rise building in large urban and successfully sustain the stresses caused by seismic load. This alternative should

take into consideration the factors of safety, low cost, durability, sustainability and productivity for constructing many low-rise building in large urban to handle the housing problems in Egypt where the majority of people can't afford new building due to its expensive costs. According to the cost of the building materials in Egypt 2016, it was found that in the large urban the cost of constructing many low-rise URM building composed of 3 storey of flat area around 300-400 m^2, would be less than the cost of the RC pairs by 25-30%. The reason of that reduction in cost is due to avoiding using steel reinforcement. Consequently, we got less overall cost in urban projects. In this study, the proposed statically systems of these buildings are composed of limestone URM wall up to 3 storeys supporting limestone URM barrel vaults with sandy backfill to guarantee topping plane floors . The footing are proposed to be strip type of limestone URM units over PC strip one. The research is focusing on the analytical analysis by using the commercial finite element program "Abaqus 6.12" [10] beside the experimental tests conducting the mechanical properties of the URM system. In our study, a ground earthquake excitation of El-Centro 1940 was analytically applied on the base of that proposed URM building and the entire building stresses were observed. Thus, a nonlinear analysis that allows for stress redistribution is more realistic for describing the actual behavior of unreinforced masonry structures and the main challenge here is the capability of these URM structures to sustain the stresses caused by the seismic loads [11].

II. F.E. MODELING

2.1. General

This paper contains the results of the analytical study conducted to evaluate the unreinforced stone masonry structures (URM) of limestone barrel vaults rested on URM walls under the seismic load and also to study the effect of both the wall thickness and vaults thickness on the URM capacity. [11] These proposed structures were considered low rise building of 3 floors. The concepts of value engineering and sustainability are considered the main goals of using this type of structures.The experimental test program was made to conduct the mechanical properties of the URM prisms and it consists of nine masonry assembly constructed with three different types of locally available limestone masonry bricks, the walls were tested under compression, tensile, shear tests according to the Egyptian code requirements (ECP204-2005) [12]. The mechanical properties for these nine assemblages were calculated such as the ultimate compressive strength, ultimate tensile strength, bond strength and young's modulus [11]. These parameters were used in the F.E. to perform parametric study on the proposed URM building.The acting stresses during the F.E. analysis were observed and be compared with the ultimate strength conducted from experimental tests to evaluate the ultimate capacity of the structure. The shell elements in the F.E. were chosen in the parametric study to model the proposed building for the macro-modeling technique [13] whereas the solid elements were used in the verification process [11].

2.2. Proposed Model Characterization

The core of this study was to introduce a type of structures with less cost. So, there was a proposal of masonry structural system composed of many URM walls supporting URM barrel vaults. This building has 3 storey in elevation (Fig. 1) where the URM height is 3200 mm between any two elevated vaults. Moreover, the plan had equal subdivided lengths and widths of the rooms. The number of rooms in plan were 4x4 and each room has dimensions assumed to be (BxL=4000x4000 mm) as in Fig. 2. In addition, indoor RC stairs of constant thickness (t_{stairs}=200 mm) were provided in the building and rested on the URM bearing walls as in Fig. 3.
The URM barrel vaults are covering the rooms and considered the floors of the building, they have a constant height of 800 mm, and their lengths and widths are equal 4000 mm., see Fig. 4. In the entire building, there are many openings forming the shapes of the windows and the doors however, the edge distance of these openings is equal 1000 mm as shown in Fig. 5. The windows are centered in each URM wall elevation with dimensions BxH=1400x1000 mm, also the doors have dimensions BxH=1000x2200 mm in Fig. 5. The backfill was sand to prepare a horizontal plane floors at each story, the superimposed load of this backfill was taken into consideration in the F.E. model.

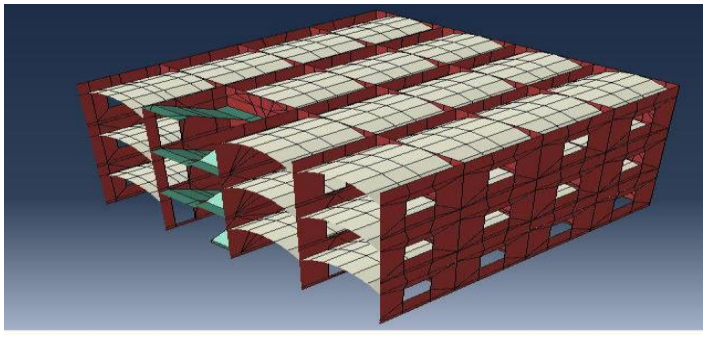

Fig. 1: Building in elevation

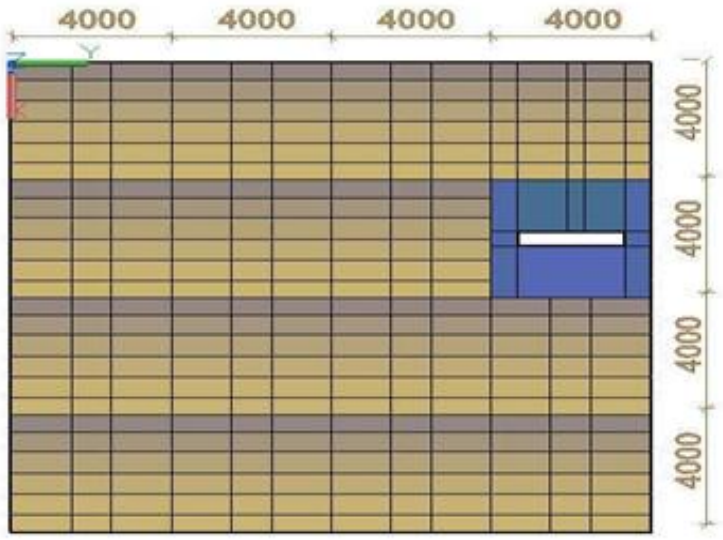

Fig. 2: Building in plan

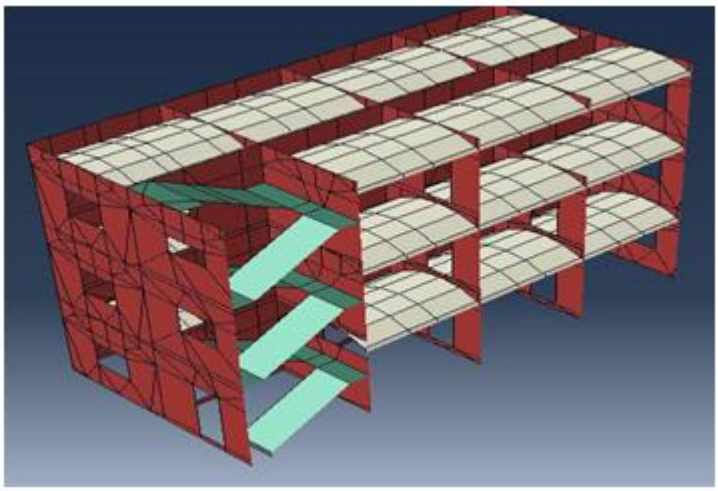

Fig. 3: Indoor reinforced concrete stairs

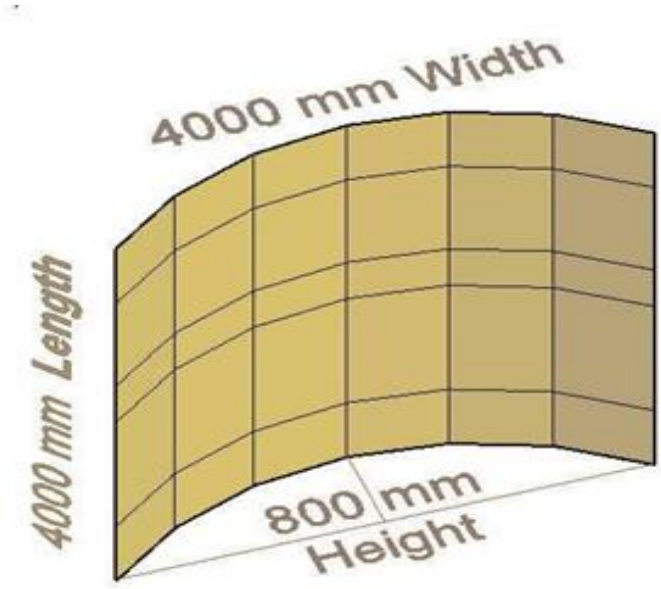

Fig. 4: URM barrel vault dimensions

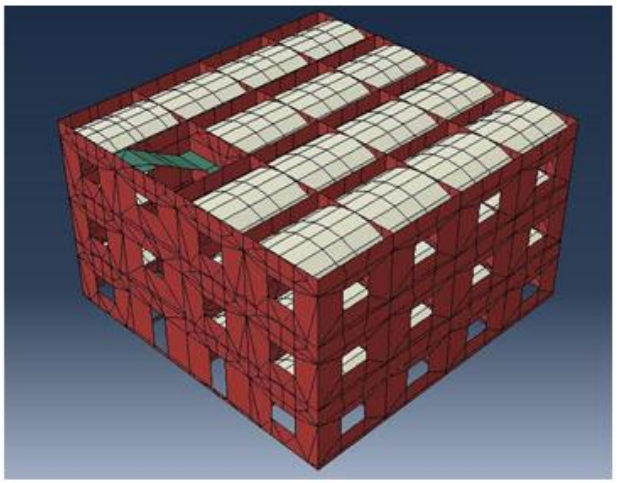

Fig. 5: Openings (windows and doors) in the entire URM building **2.3. Types of the applied loads in the F.E. model**

In this model, the loads factors were equal 1 and were categorized into 3 types:

1. Gravity loads including own weight and the superimposed sand backfill as shown in Fig. 6.
2. Nonlinear time history due to the earthquake record of El-Centro 1940 (Fig.7) to be the ground excitation with duration =30.4 seconds where the point of application was at the base level of the building as shown in Fig.6.

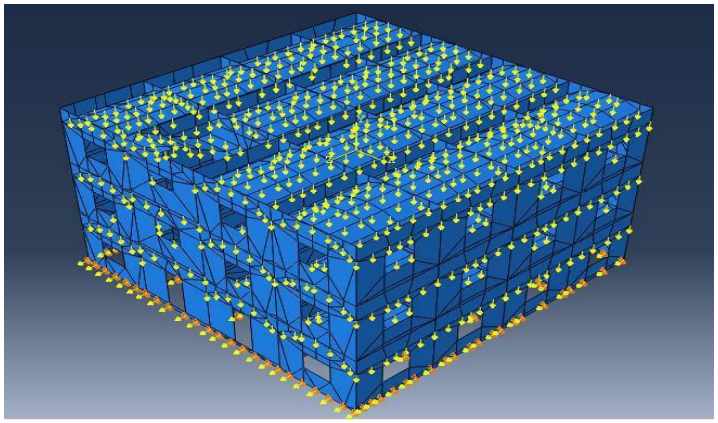

Fig. 6: Applied gravity loads in the F.E. model

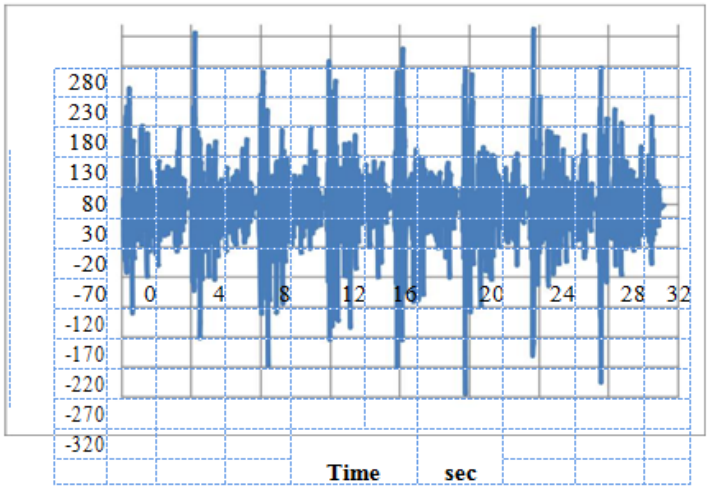

Fig. 7: Record of El-Centro (1940) Earthquake

2.4. Material Characterization

A lot of research has been carried out on the F.E. of masonry structures, considering the complexity arising from the fact that masonry is an anisotropic composite material. The most of these models treat masonry, either as an ideal homogeneous material with constitutive equations that differ from those of the components, or two-phase material models where the components are considered separately to account for the interaction between them. These approaches are reported frequently as “macro modelling” or “micro modeling. In our study, the material was considered an "equivalent" masonry (homogenized material), furthermore, the macro-modeling technique [13] was developed in all the parametric study after was verified in chapter

4. The density was inserted $\boldsymbol{\rho}$ = 0.175 kg/m^3, poisson's ratio $\boldsymbol{\upsilon}$ was taken 0.30 and the young's modulus was experimentally computed in compression test with value **E**=780 MPA. In the compression behavior, the stress-strain curve was input besides no tension recovery $\mathbf{w_t}$=0, whereas, the tension behavior had its own stress-strain curve with compression recovery $\mathbf{w_c}$=0.

2.5. Shell element used in the F.E. model

It was decided to use shell element S4R from Abaqus 6.12 F.E. library [10] to be the element representing all the URM walls and vaults. It was considered three-dimensional element of 4 nodes and reduced integration. For shells in space the positive normal is given by the right-hand rule going around the nodes of the element in the order that they are specified in the element definition as shown in Fig. 8.

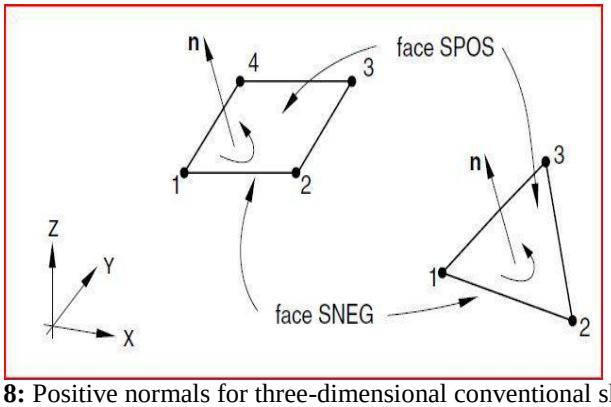

Fig. 8: Positive normals for three-dimensional conventional shells.

3. Parametric Study

Each F.E. model consists of 2824 shell elements and 16971 nodes, knowing that the all vaults direction was the same direction of the ground excitation, it was decided to choose two variable parameters to be the cases of study;

1. Wall Thicknesses are 250,300,350,400 and 450 mm.
2. Vault Thicknesses are 130,260 and 390 mm.

Five critical control points were used to monitor the ultimate stresses and responses, control point (1) was mainly monitoring the maximum compression stresses $\boldsymbol{\sigma_c}$, control point (2) was mainly used to capture the maximum tensile stresses $\boldsymbol{\sigma_t}$, control point (3) was to get the maximum shear stresses $\boldsymbol{\tau}$, control point (4) was illustrating the maximum of both the displacement **u** and velocity **ú**, and finally control point (5) was to record the maximum acceleration **ü**. The locations of these control points are mentioned in Fig. 9, 10.

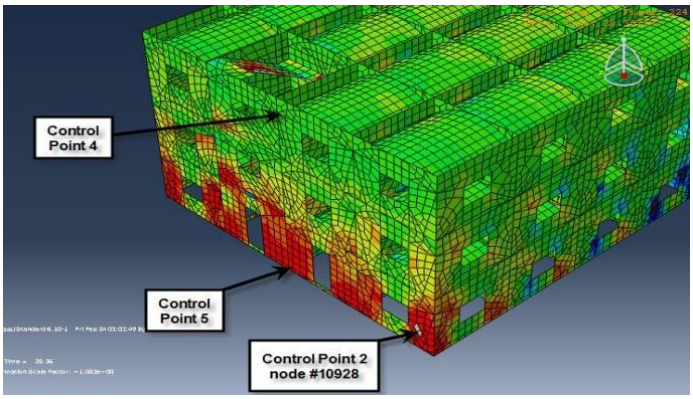

Fig. 9: Locations of the chosen control points 2, 4&5.

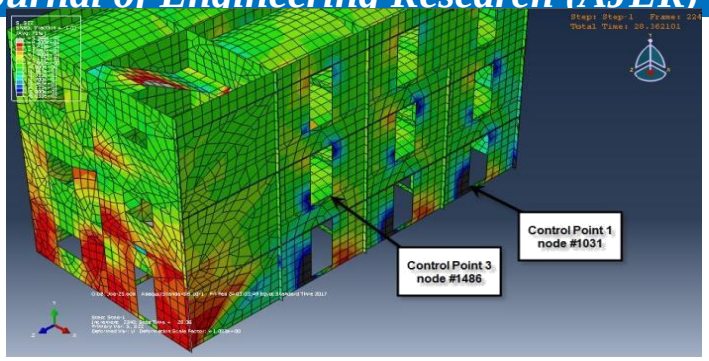

Fig. 10: Locations of the chosen control points 1&3.

3.1. VARIABLE WALL THICKNESSES (250,300,350,400 and 450 mm.)

In RUN-1, the first study case, the boundary conditions were input in the Abaqus F.E. model at the base level in the initial step. Moreover, the nonlinear time history analysis was performed and the ground acceleration of El-Centro earthquake was applied at the base level with its whole time history of 30.4 seconds in the next step beside the gravity loads. The mesh size configuration was built as shown in Fig. 11 with mesh size around 400 mm. The direction of earthquake excitation was indicated in the same Fig. 11.

For control point (1) or (node 1031) in the inner wall: Figures 12, 13 are showing that the maximum compressive stress σ_c =1.516 MPa (35.42% the ultimate compressive strength) at time 16.546 seconds while the max. σ_c =0.46 MPa at another corresponding point (node 188) at the outer wall in the same level (i.e. reduced by 69.65%). The other F.E. runs ensure what happened and could be explained that the inner wall had larger mass than the outer wall so that the max. σc in the inner wall were larger than the max. σ_c in the outer wall. That reason could lead us to design the inner walls to be thicker than the outer ones.

Another note could be seen that the max. σ_c in the inner wall occurred at the sharp corner of the door opening which is meaning that corner would better behave if it was curved and higher little more above the base level to avoid the existing of the stress concentration.

For control point (2) (i.e. node 10928): Figures 14, 15 show that the maximum tensile stress σ_t was 0.510 MPa (95.32% the ultimate tensile strength) at time 4.28 sec. Despite the tensile stresses were critical, but they did not exceed the ultimate limit where the other F.E. runs ensured what took place. We can figure out that the masonry structure could sustain these stresses. The heritage masonry building could safely along thousands years ago resist the tensile stresses due to seismic loads. Moreover, they had not collapsed and remain safe and stable till present. The reason may be that some kind of the stresses distribution occurred when the tensile stresses about just reach the ultimate capacity. In addition, the nonlinear analysis always gives more resistance more than conservative linear analysis.

For control point (3) (i.e. node 1486): Figures 16, 17 show that the maximum shear stress τ was 0.665 MPa (20.78% the ultimate shear strength) at time 8.57 sec. For control point (4): Figures 18, 19 and 20 show the deformed shape occurred when the maximum displacement was 1.489 m at time 28.673 sec. , the maximum velocity was 0.32 m/sec at 4.38 sec. For control point (5): Figure 21 is showing the acceleration response of the building.

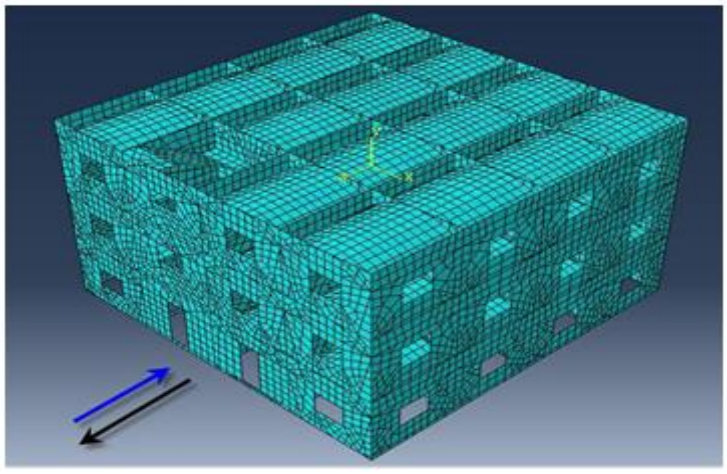

Fig. 11: RUN 1- Mesh Configuration

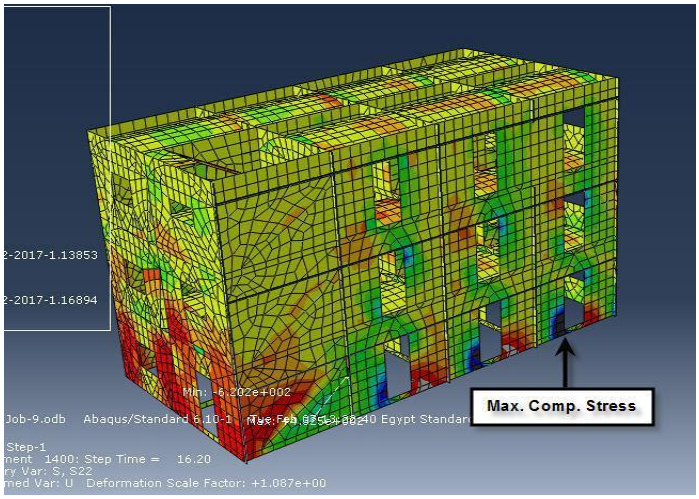

Fig.12: Max. σ_c = 1.516 MPa at 16.546 sec.

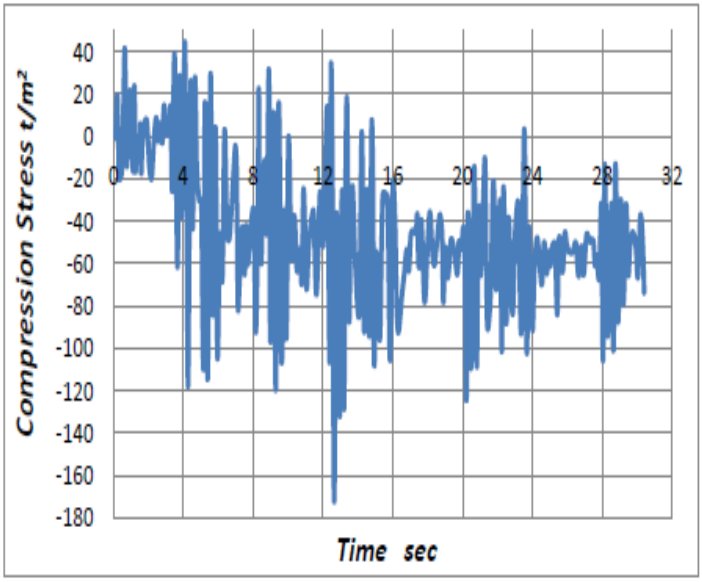

Fig. 13: Results of Control point (1)

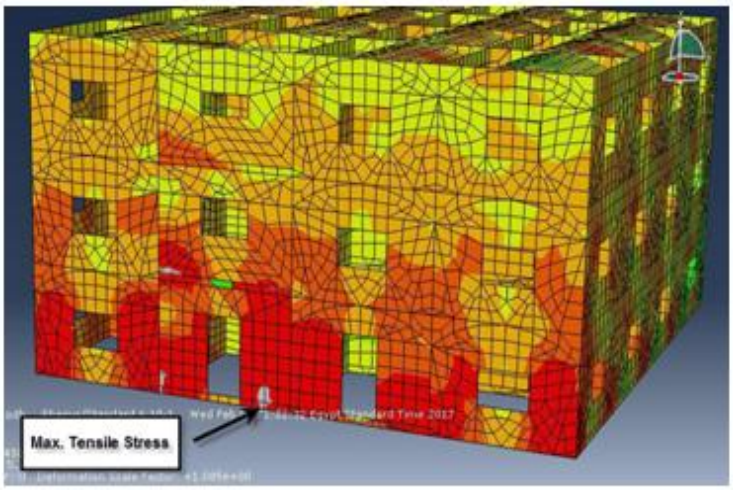

Fig.14: Max. σ_t = 0.510 MPa at 4.28 sec.

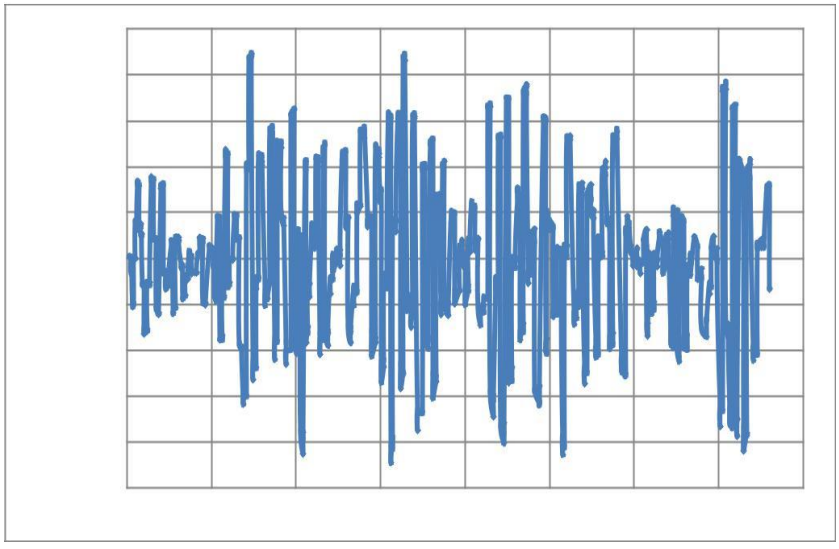

Fig. 15: Results of Control point (2)

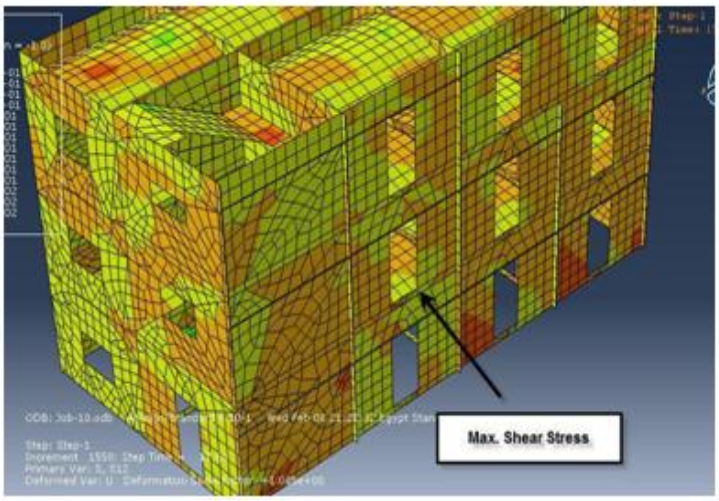

Fig. 16: Max. τ= 0.665 MPa at 8.57 sec.

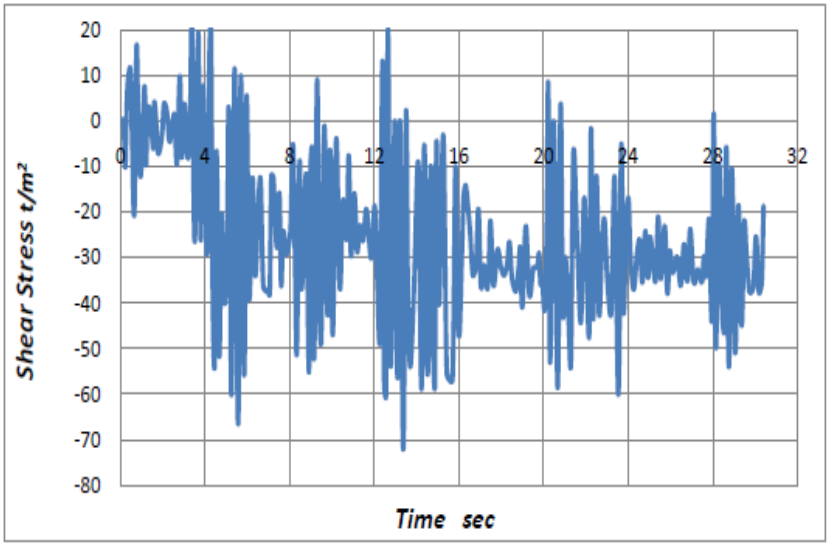

Fig. 17: Results of Control point (3)

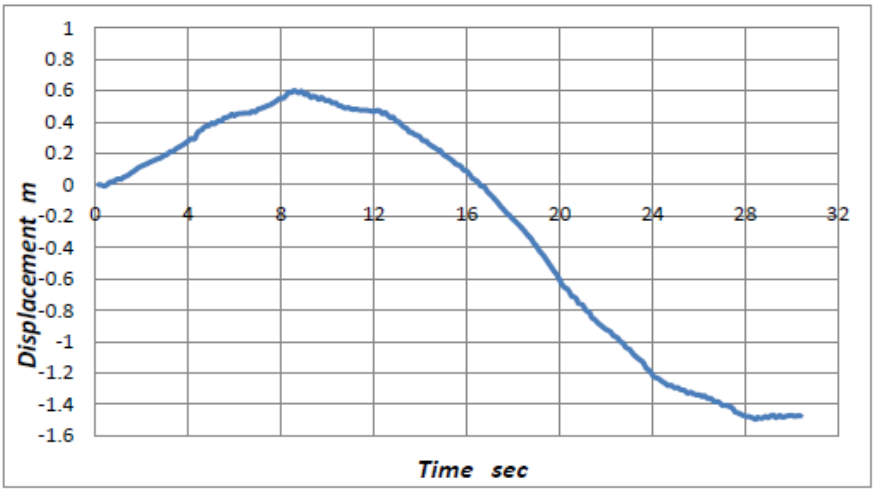

Fig. 18: Displacement response u of Control point (4)

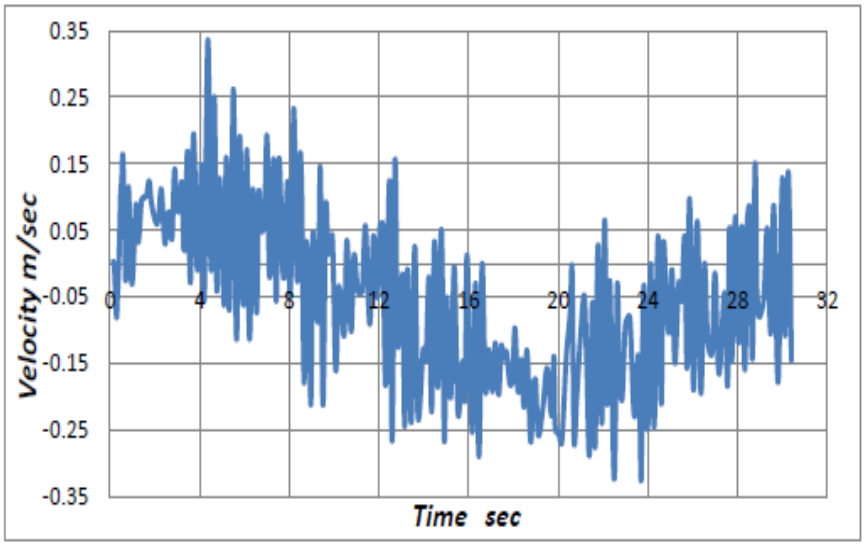

Fig. 19: Velocity response ***ú*** of Control point (4)

Fig. 20: Deformed shape $\mathbf{U_3}$ at the max. Displacement

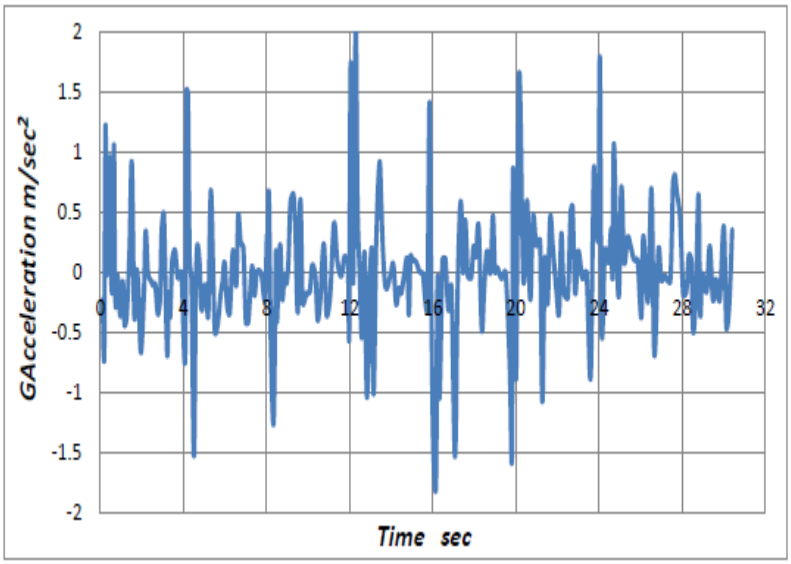

Fig. 21: Acceleration response $\ddot{u}$ at the base- Control point (5)

The rest of modeling runs can be summarized in the next tables here, the results related to the maximum compressive stress σ_c at the control point 1 (node 1031) in the inner wall and also obtained from the five runs as shown in the next Table 1, however, the max. σ_t at the same node was observed to evaluate both compressive and tensile stresses

tvault/twall	twall/Lroom	tvault/Lroom	Time of Max. σ_c (sec.)	Max. σ_c MPa	Time of max. σ_t	Max. σ_t MPa
130/250=0.52	250/4000=0.0625	130/4000=0.0325	16.546	1.516	0.492	0.642
130/300=0.433	300/4000=0.075	130/4000=0.0325	13.14	1.602	0.429	7.39
130/350=0.371	350/4000=0.0875	130/4000=0.0325	28.389	1.923	0.434	25.026
130/400=0.325	400/4000=0.10	130/4000=0.0325	12.64	1.718	0.4228	4.075
130/450=0.288	450/4000=0.1125	130/4000=0.0325	28.36	1.339	0.428	27.63

Table 1: Summary of the Max. Values of σ_c due to variable wall thicknesses

From previous Table 1, it was noted that if the wall thickness increased from thickness 250 mm up to thickness 350 mm, the Max compressive stresses σ_c increased, but if the thickness was more than 350 mm, the σ_c would be decrease. It perhaps because that the impact of the mass of walls was more effective than the impact of their thickness (i.e. geometry).Whereas, after increasing wall thickness more than 350 mm, the crass sectional area (geometry) had the largest effect than increasing mass of walls. The large cross sectional area would govern the behavior in this case. Also, it was clearly noticed that the proposed URM could safely sustain the maximum compressive stresses with the shown safety margin in Table 2:

tvault/twall	twall/Lroom	tvault/Lroom	Max. σ_c MPa	Ultimate Comp. Strength MPa	% Safety Margin
130/250=0.52	250/4000=0.0625	130/4000=0.0325	1.516	4.28	35.42
130/300=0.433	300/4000=0.075	130/4000=0.0325	1.602	4.28	37.43
130/350=0.371	350/4000=0.0875	130/4000=0.0325	1.923	4.28	44.92
130/400=0.325	400/4000=0.10	130/4000=0.0325	1.718	4.28	40.14
130/450=0.288	450/4000=0.1125	130/4000=0.0325	1.339	4.28	31.28

Table 2: % Safety Margin for the Max. σ_c for variable wall thicknesses

The next Table 3 is monitoring the relation differences between σ_c & σ^*_c where σ^*_c was the Maximum compression stress at another corresponding node (188) at the same level but located in the outer wall. The fact announced on increasing inner walls more than the outer walls was significantly proper and should be adopted in any further studies. Nevertheless, the maximum tensile stress at control point 2 (node 10928) of the previous analytical models can be briefly stated below in Table 4.

tvault/twall	twall/Lroom	tvault/Lroom	Max. σ_c Node (1031)	Max. σ^*_c Node (188)	% Safety Margin
130/250=0.52	250/4000=0.0625	130/4000=0.0325	1.516	0.46	69.65
130/300=0.433	300/4000=0.075	130/4000=0.0325	1.602	0.666	58.42
130/350=0.371	350/4000=0.0875	130/4000=0.0325	1.923	0.814	57.67
130/400=0.325	400/4000=0.10	130/4000=0.0325	1.718	0.59	65.65
130/450=0.288	450/4000=0.1125	130/4000=0.0325	1.339	0.552	58.77

Table 3: Summary of the Max. Values of σ_c & σ^*_c due to variable wall thicknesses

tvault/twall	twall/Lroom	tvault/Lroom	Max. σ_t Node (10928)	At Time (sec.)	% Margin
130/250=0.52	250/4000=0.0625	130/4000=0.0325	0.510	4.28	95.32
130/300=0.433	300/4000=0.075	130/4000=0.0325	0.451	13.143	84.29

130/350=0.371	350/4000=0.0875	130/4000=0.0325	0.4462	27.988	83.40
130/400=0.325	400/4000=0.10	130/4000=0.0325	0.4268	4.27	79.775
130/450=0.288	450/4000=0.1125	130/4000=0.0325	0.416	27.705	77.75

Table 4: Summary of the Max. Values of σ_t due to variable wall thicknesses

From Table 4, it was significantly shown that the more wall thickness increased, the less tensile stresses occurred. Therefore, according to the nonlinear analysis, the stresses did not exceed the ultimate limit experimentally conducted. In fact, it exceeds the linear conservative limit according to the Egyptian code but if we adopted this linear limit, the masonry structures would be too limited and not widely spread whereas the heritage masonry structures and momentums had experienced many historic seismic records over thousands years without any failure or presence of the cracks. However, the linear conservative limit may be revised to help us use untraditional safe, durable and economic low-rise building.

The analytical analysis was regarding the shear stresses in the walls that meshed as macro-modeling technique. These stresses did not exceed the ultimate capacity of the assembly experimentally tested (Modified Triplet Test) in the MRC lab. The safety margin was large and beneath 20%. The conducted reason here is that the walls had behaved as deep shear wall. Moreover, the shear stresses were resisted by a large bed joint cross section area. However, the stress concentration was developed at the sharp edge of the openings which is leading us to adopt curved and smooth opening corners, thus would contribute to minimize the local shear stress concentrations. In addition, with wall thicknesses less than 350mm, the shear stresses τ increased. On contrary, τ decreased after with wall thickness larger than 350 mm. Furthermore, it can be noted that the base shear was earlier affected by the increasing the wall mass more than the wall geometry when the wall thickness was less than 350 But, when the wall thickness increased more than 350 mm, the geometry would be more effective than the wall mass to govern the shear stresses behavior and reduce these stresses when the wall thickness increased larger than 350 mm. Table 5 is showing the results observed for the monitoring the Max. τ stresses. Also, the peak displacement was observed at control point (4) and it was found a slight change in its value with variation of the wall thicknesses in nearly the same times. Table 6 is presenting these values with its time occur.

tvault/twall	twall/Lroom	tvault/Lroom	Max. (τ) Node (1486) MPa	Ultimate Shear Strength MPa	At Time (sec.)	% Safety Margin
130/250=0.52	250/4000=0.0625	130/4000=0.0325	0.665	3.20	8.577	20.78
130/300=0.433	300/4000=0.075	130/4000=0.0325	0.767	4.516	13.27	16.98
130/350=0.371	350/4000=0.0875	130/4000=0.0325	0.975	5.05	28.919	19.30
130/400=0.325	400/4000=0.10	130/4000=0.0325	0.7129	3.598	13.37	19.81
130/450=0.288	450/4000=0.1125	130/4000=0.0325	0.7324	3.861	28.45	18.969

Table 5: Summary of the Max. τ due to variable wall thicknesses

tvault/twall	twall/Lroom	tvault/Lroom	Max. displacement u (m)	At Time (sec.)
130/250=0.52	250/4000=0.0625	130/4000=0.0325	1.489	28.673

130/300=0.433	300/4000=0.075	130/4000=0.0325	1.492	28.30
130/350=0.371	350/4000=0.0875	130/4000=0.0325	1.5027	28.38
130/400=0.325	400/4000=0.10	130/4000=0.0325	1.490	28.64
130/450=0.288	450/4000=0.1125	130/4000=0.0325	1.497	28.36

Table 6: Summary of the Max. (u) for variable wall thicknesses **3.2. VARIABLE VAULT THICKNESSES (130,260,390 mm.)**

In the second variable parametric study, the vault thickness=260mm, and looking for the control point (1): the maximum σ_c was 1.871 MPa (43.714% the ultimate compressive strength) at time 27.988 seconds. It was noted that there is an increase in the value of σ_c when the vault thickness was duplicated. Therefore, we can figure out that the mass was duplicated and incorporated in this increase of compression stresses due to both of the axial normal forces beside the bending stresses due to the overturning moments from the time history analysis. The corresponding Node (188) located at the same position but in the outer wall experienced σ_c=0.885 MPa which ensures that the inner walls should be thicker than the outer walls according to these results. For the same control point (1), the maximum σ_t was 0.403 MPa (75.32% the ultimate tensile strength) at time 24.19 sec.

For control point (2): it was shown that the maximum tensile stress σ_t was 0.4488 MPa (83.88% the ultimate tensile strength) at time 27.988 sec. This value of σ_t was higher compared to the value of the same node when the vault thickness was duplicated. Consequently, it figures out that the overturning moments due to the duplicated mass in the time history period had essentially incorporated in that mentioned issue. It was expected that the enhancement in both framing actions and rigidity of the diaphragm vaults would lead to reduce the maximum tensile stresses σ_t but, the behavior was on contrast. However, the both max. σ_c and σ_t were beneath the ultimate values. For control point (3): the maximum shear stress τ was 0.876 MPa (17.91% the ultimate shear strength) at time 29.187sec. The base shear significantly increased due to the duplicated mass vault in that trial analysis. Therefore, it is not recommended to increase the vault thickness to avoid the increase of σ_c , σ_t and τ.

For control point (4): the deformed shape occurred when the maximum displacement was 1.50 m at time 28.20 sec. All these results from the second parameter "vault thickness" can be summarized here in the coming Tables 7 to 12.

tvault/twall	twall/Lroom	tvault/Lroom	Time of Max. σ_c (sec.)	Max. σ_c MPa	Time of Max. σ_t MPa	Max. σ_t MPa
130/400=0.325	400/4000=0.10	130/4000=0.0325	12.64	1.718	0.4228	4.075
260/400=0.650	400/4000=0.10	260/4000=0.065	27.988	1.871	0.403	24.19
390/400=0.975	400/4000=0.10	390/4000=0.0975	24.089	2.044	0.4417	27.875

Table 7: Summary of the Max. Values of σ_c due to variable vault thicknesses

tvault/twall	twall/Lroom	tvault/Lroom	Max. σ_c MPa	Ultimate Comp. Strength MPa	% Safety Margin
130/400=0.325	400/4000=0.10	130/4000=0.0325	1.718	4.28	40.14
260/400=0.650	400/4000=0.10	260/4000=0.065	1.871	4.28	43.71
390/400=0.975	400/4000=0.10	390/4000=0.0975	2.044	4.28	47.75

Table 8: Safety Margin for the Max. σ_c for variable vault thicknesses

			Max. σ_c	Max. σ^*_c	% Safety

tvault/twall	twall/Lroom	tvault/Lroom	Node (1031)	Node (188)	Margin
130/400=0.325	400/4000=0.10	130/4000=0.0325	1.718	0.59	34.34
260/400=0.650	400/4000=0.10	260/4000=0.065	1.871	0.8855	47.32
390/400=0.975	400/4000=0.10	390/4000=0.0975	2.044	0.870	42.56

Table 9: Summary of the Max. Values of σ_c & σ^*_c due to variable vault thicknesses

tvault/twall	twall/Lroom	tvault/Lroom	Max. σ_t Node (10928)	At Time (sec.)	% Margin
130/400=0.325	400/4000=0.10	130/4000=0.0325	0.4268	4.27	79.77
260/400=0.650	400/4000=0.10	260/4000=0.065	0.4488	27.988	83.88
390/400=0.975	400/4000=0.10	390/4000=0.0975	0.4517	19.2452	84.43

Table 10: Summary of the Max. Values of σ_t due to variable vault thicknesses

tvault/twall	twall/Lroom	tvault/Lroom	Max. τ Node (1486) MPa	Ultimate Shear Strength MPa	At Time (sec.)	% Safety Margin
130/400=0.325	400/4000=0.10	130/4000=0.0325	0.7129	3.598	13.376	19.81
260/400=0.650	400/4000=0.10	260/4000=0.065	0.876	4.89	4.89	17.91
390/400=0.975	400/4000=0.10	390/4000=0.0975	0.859	5.216	27.875	16.468

Table 11: Summary of the Max. τ due to variable wall thicknesses

tvault/twall	twall/Lroom	tvault/Lroom	Max. displacement u (m)	At Time (sec.)
130/400=0.325	400/4000=0.10	130/4000=0.0325	1.490	28.64
260/400=0.650	400/4000=0.10	260/4000=0.065	1.5003	28.446
390/400=0.975	400/4000=0.10	390/4000=0.0975	1.5013	28.468

Table 12: Summary of the Max. (u) for variable vault thicknesses

III. SUMMARY AND CONCLUSIONS

The main challenge here is the capability of these URM structures to sustain seismic loading without any serious damage or cracks. So the cases of study will emphasis this concept after performing a nonlinear time history analysis in all the F.E. models. An earthquake record of El-Centro 1940 will be analytically conducted by using a commercial F.E. program (Abaqus 6.12) to study the variable geometry and material parameters, the stresses and the drifts resulted in such dynamic time history record. This thesis demonstrates both analytical and experimental investigations of the nonlinear behavior of unreinforced masonry vaults which is mean ultimate failure. Usually, linear analysis is conducted for simplifying analysis and design of masonry structures by using load and strength factors. However, such simplification might underestimate the structural capacity of these constructions in many cases, and thusthe nonlinear analysis gives better description for the actual behavior and capacity of the structure. The mechanical properties of such building material are conducted from the experimental tests in the Lab.

The main problem faced by the design of masonry structures through linear analysis is that tension stresses usually exceed the masonry tensile stresses allowed by most design codes. Usually, wall thickness will be increased or steel reinforcement will be provided at these locations. However, evidence proves that these structures are quite safe, as similar masonry structures are observed to survive for very long ages and not collapse or even show visible cracks. This may be attributed to the fact that the stresses are redistributed within the structural element after the tensile stresses reach the limiting value for masonry. Thus, a nonlinear analysis that allows for stress redistribution is more realistic for describing the actual behavior of unreinforced masonry structures. The objective of this study is to demonstrate the efficiency and ease of application of the adopted numerical modeling to reliable design of new structures made of load bearing masonry elements. The proposed model is applied for the URM low-rise building of 3 strory to be practical economic choice instead of RC structures for constructing many buildings in large urban.

Some conclusions can be obtained here from this comprehensive parametric study. First, all the F.E. models proved that the proposed URM low-rise building did not exceed the ultimate compressive, tensile and shear stresses. That would lead us to adopt the mentioned masonry system to be a practical alternative instead of the RC or steel low-rise building. Second, it was demonstrated that the limit for tensile strength determined from the nonlinear analysis model was 0.535 MPa. This limit represents a ratio of 0.125 of compressive strength, which is within the range found in text books and reported by researchers as previously stated. Failure loads of prisms T1, T2 and T3 numerically predicted using this tensile limit, were verified experimentally. The Egyptian code allowable tensile stress along bed joints is equal to 0.07 MPa, which is only 13% of the ultimate tensile stress obtained in the experimental results. This low limit for tensile and also compressive stresses specified in ECP underestimates the capacity of masonry structures which may imply a doubting atmosphere and limit the wide application of load-bearing masonry structures in major engineering projects, in spite of all its benefits from the structural, environmental and economic points of view [2].

Third, despite the tensile stresses were critical, but they did not exceed the ultimate limit where the other F.E. trials ensured what took place. We can figure out that the masonry structure could sustain these stresses. The heritage masonry building could safely along thousands years ago resist the tensile stresses due to seismic loads. Moreover, they had not collapsed and remain safe and stable till present. The reason may be that some kind of the stresses distribution occurred when the tensile stresses about just reach the ultimate capacity. In addition, the nonlinear analysis always gives more resistance more than conservative linear analysis. Forth, all F.E. performed models in this study ensured that the max. σ_c in the inner wall were larger than the max. σ_c in the outer wall due to the relative served mass for each wall where the inner had the bigger mass value. Therefore, the inner walls should be thicker than the outer ones.

Fifth, it was clearly observed that the max. σ_c in the inner wall occurred at the sharp corner of the door opening which means that corner effect would better behave if it was curved and higher little more above the base level to avoid the existing of the stress concentration. Sixth, the F.E. models cleared that it was no need to increase the wall thickness bigger more than 130 mm, the nominal commercial limestone brick thickness. In spite of the benefits of getting more rigid vault diaphragm and getting more framing action criteria, but it is not recommended to increase the vault thickness to avoid any increase in compressive, tensile and shear stresses.

RECOMMENDATIONS

1. More sophisticated studies should be made for the fracture in the masonry low-rise building. A combination of FEM and DEM would be helpful to achieve that target.
2. More studies should take into consideration the effect of changing the room modules in plan to be larger or smaller than 4000x4000mm.
3. Changing the vault orientation may cause some effects on structure behavior for both stresses and deformations results.

4. The thermal isolation property against the hot and cold weather should be studied.
5. Further future studies should concern the relation between footing and the URM walls.
6. Changing the clear height of each story will probably imply the masonry behavior against the lateral loads.
7. Proper washing for the limestone units should results in better structural behavior and performance since the harmful substances of bad effects on mortar are removed.
8. URM low-rise building should be widely used in housing urban to solve the problems of a certain people class that cannot afford the apartments.
9. Also this type of building can be constructed in the emergency circumstances to be temporary residences if the natural catastrophic disasters occurred.

ACKNOWLEDGEMENT

I would like to express my deepest thanks and appreciation to my supervisor, Prof. Dr. Abdelsalam Mokhtar for his guidance and advice throughout this work. I am grateful to him all for having the opportunity to work under his supervision. Also, I would like to Prof. Dr. Gamal Hussein for his great help in this work. Special thanks for my supervisors; Dr. Mahmoud Elghorab and Dr. Mohamed Kohail Fayez for their valuable assistance, guidance, patience and endless support throughout this research, and reviewing of the manuscript are greatly acknowledged. The experimental work was carried out at the Material Research Centre (MRC) of the Structural Engineering Department at Ain-Shams University. The help of the laboratory technicians in developing work is greatly appreciated for their distinguished assistance during the experimental work. Finally, I would like to thank my parents and my wife for their continuous support, filling me with hope and enthusiasm, especially during the hard times.

REFERENCES

[1]. A. Giordano, E. Mele, A. De Luca, Modelling of historical masonry structures: comparison of different approaches through a case study, Eng. Struct. 24 (8) (2002) 1057–1069.
[2]. O.A. Kamal et al., Nonlinear analysis of historic and contemporary vaulted masonry assemblages, HBRC Journal (2013)
[3]. A.A. Hamid, How to face the increasing cost of reinforcing steel in RC frame construction in Egypt, Keynote lecture, in: Workshop of Proposed Alternatives to Face the Increasing Cost of Steel Reinforcement Used in RC Structures in Egypt, Housing and Building Research Center, Cairo, Egypt, 2006 (January 2).
[4]. R. Eldahan, M.I. Saafan, Low cost housing, in: Workshop on Economic Challenges to Reduce Building Costs, Housing and Building Research Center, Cairo, Egypt, 2008.
[5]. Clough, R. H., Mayes R. L. and Gulkan, P. (1979). Shaking Table Study of Single-Story Masonry Houses, Vol.3: Summary, Conclusions, and Recommendations. Report No. UCB/EEERC-79/25, University of California, Berkeley, CA.
[6]. Costley, A.C. and Abrams, D.P. (1996). Dynamic Response of Unreinforced Masonry Buildings with Flexible Diaphragms. NCEER-96-0001, University of Buffalo,Buffalo, N.Y.
[7]. Magenes, G., Kingsley, G. R., and Calvi, G. M (1995). Seismic Testing of a Full-Scale, Two-story Masonry Building: Test Procedure and Measured Experimental Response, in Experimental and Numerical Investigation on a Brick Masonry Building Prototype. Report 3.0, Gruppo Nazionale La Difesa Dai Terremoti.
[8]. Moon, F., Yi, T., Leon, R. and Kahn, L. (2003). Large-Scale Tests of an Unreinforced Masonry Low-Rise Building. Ninth North American Masonry Conference, Clemson, SC.
[9]. Paquette J. and Bruneau, M. (1999). Seismic Resistance of Full Scale Single Story Brick Masonry Building Specimen. 8th North American Masonry Conference, June 6-9, Austin, Texas, pp. 227-234.
[10]. Abaqus CAE 6.12, User's and Theory Manuals.
[11]. Elsayem M.G., PERFORMANCE ASSESSMENT OF MULTI STORY STONE UNREINFORCED MASONRY BUILDINGS WITH BARREL VAULTS UNDER SEISMIC LOADS (PhD. thesis), Faculty of Engineering at Ain Shams University, 2017.
[12]. ECP204-2005, Egyptian Code for Design of Masonry Structures, Housing and Building Research Center, Ministry of Housing Utilities and Urban Communities, Egypt, 2005.
[13]. Lourenco, P.B. (1996). Computational Strategies for Masonry Structures. Delft University Press, the Netherlands.

*Mohamed Gamaleldeen Elsayem. " Performane Assessment of Unreinforced Masonry Low-Rise Building Composed of Limestone Bricks Under Seismic Loading " American Journal of Engineering Research (AJER) 6.7 (2017): 347-363.